HHS Public Access

Author manuscript

Am J Med Genet A. Author manuscript; available in PMC 2023 April 07.

Published in final edited form as:

Am J Med Genet A. 2016 November ; 170(11): 3028–3032. doi:10.1002/ajmg.a.37847.

Increased bone turnover, osteoporosis, progressive tibial bowing, fractures, and scoliosis in a patient with a final-exon *SATB2* frameshift mutation

Philip M. Boone, M.D., Ph.D.[1], **Yiu Man Chan, M.R.C.O.G.**[2], **Jill V. Hunter, M.D.**[3], **Louis E. Pottkotter, M.D.**[3], **Nelson A. Davino, M.D.**[4], **Yaping Yang, Ph.D.**[1,3], **Joke Beuten, Ph.D.**[1,5], **Carlos A. Bacino, M.D.**[1,3,5,*]

[1)]Dept. of Molecular and Human Genetics, Baylor College of Medicine, Houston, TX, USA

[2)]Dept. of Obstetrics and Gynaecology, Chinese University of Hong Kong, Hong Kong, People's Republic of China

[3)]Texas Children's Hospital, Houston, TX, USA

[4)]Memorial Hermann Hospital, Katy, Texas, USA

[5)]Baylor Miraca Genetics Laboratories, Baylor College of Medicine

Abstract

Haploinsufficiency of *SATB2* causes cleft palate, intellectual disability with deficient speech, facial and dental abnormalities, and other variable features known collectively as *SATB2*-associated syndrome. This phenotype was accompanied by osteoporosis, fractures, and tibial bowing in two previously reported adult patients; each possessed *SATB2* mutations either predicted or demonstrated to escape nonsense-mediated decay, suggesting that the additional bone defects result from a dominant negative effect and/or age-dependent penetrance. These hypotheses remain to be confirmed, as do the specific downstream defects causing bone abnormalities. We report a *SATB2* mutation (c.2018dupA; p.(H673fs)) in a 15-year-old patient whose *SATB2*-associated syndrome phenotype is accompanied by osteoporosis, fractures, progressive tibial bowing, and scoliosis. As this homeodomain-disrupting and predicted truncating mutation resides within the final exon of *SATB2*, escape from nonsense-mediated decay is likely. Thus, we provide further evidence of bone phenotypes beyond those typically associated with *SATB2*-associated syndrome in individuals with potential dominant-negative *SATB2* alleles, as well as evidence for age-dependence of bone features. Elevations in alkaline phosphatase, urinary N-telopeptide/creatinine ratio, and osteocalcin in the patient indicate increased bone turnover. We propose surveillance and treatment with osteoclast inhibitors to prevent fractures and to slow progressive bone deformities.

[*]Correspondence: Dr. Carlos A. Bacino, Texas Children's Hospital, Clinical Care Center, Room 1560, MS: 225, 6701 Fannin St., Houston, TX 77030, USA, Tel: +1 832 822 4391, Fax: +1 832 825 4294, cbacino@bcm.edu.

DISCLOSURE DECLARATION

The Baylor College of Medicine Department of Molecular and Human Genetics derives revenue from molecular genetic testing in the Baylor Miraca Genetics Laboratories.

Keywords

SATB2 ; bone remodeling; osteoclastic activity; tibial bowing; Glass syndrome

INTRODUCTION

SATB2 (special AT-rich sequence binding protein 2), the product of the *SATB2* gene, is a transcriptional regulatory protein with importance to craniofacial and central nervous system development and a putative role in osteoblast development [Zhao et al., 2014]. *SATB2*-associated syndrome (SAS), the phenotype resulting from mutations affecting *SATB2* alone, has been described in patients with heterozygous whole or partial deletions [Rosenfeld et al., 2009], intragenic duplications [Lieden et al., 2014], and point mutations in *SATB2* [Leoyklang et al., 2007]. *SATB2*-associated syndrome is characterized by cleft or high palate, intellectual disability (ID) with limited speech, and dentofacial abnormalities.

Interestingly, two patients have been described in which SAS was accompanied by osteoporosis, fractures, and tibial bowing: a 36-year-old man with a nonsense (c.715C>T; p.(R239X)) mutation in exon 7 of *SATB2* [Leoyklang et al., 2007]; and a 20-year old man with an intragenic *SATB2* duplication [Lieden et al., 2014]. The *SATB2* variant described by Leoyklang et al. [2007], p.(R239X), yielded detectable mutant RNA (c.715C>T) [Döcker et al., 2014; Leoyklang et al., 2007], indicating a failure of nonsense-mediated decay (NMD). Furthermore, truncated SATB2 containing amino acids 1-238 has a dominant negative effect [Leoyklang et al., 2013], potentially explaining the additional bone features described by Leoyklang et al. [2007] compared to typical patients with *SATB2* deletion. The intragenic duplication described by Liedén, et al. [2014] is in-frame and also not expected to undergo NMD. Any genotype-phenotype correlation remains to be established, as do the downstream defects leading to additional phenotypes (i.e., failed bone development or increased bone resorption). Furthermore, treatment of this condition remains to be discussed in the literature.

CLINICAL REPORT

The patient was a 15-year-old male of Western European descent, born at 3.97 kg (75^{th}-90^{th} centile) to healthy parents following an uneventful pregnancy. Neonatal problems included feeding difficulties caused by a cleft palate, repaired at age 8 months, and middle ear fluid discovered after an abnormal hearing screen. In early childhood, the patient had global developmental delay, most severely in speech. He sat unaided at 9 m, walked at ~1 y 6 m, and never attained words. At 1 y 9 m, he had central hypotonia, peripheral spasticity, and uncoordinated walking. Early medical history also included strabismus surgery (esotropia; age 1 y); multiple tympanostomy tubes for otitis media (most recently at age 14 y); velopharyngeal insufficiency resulting in dysphagia with silent aspiration, laryngeal penetration, and nasopharyngeal regurgitation confirmed at age 6 y; ataxic gait and abnormal movements; allergic rhinitis; nasal vocalizations; and low weight (Fig. 1d). He has had at least five fractures secondary to falls, involving the clavicle (four different fractures by age 5 y) and pelvis (age 6-7 y). Finally, he has exhibited a non-painful, progressive

bowing of the lower legs noticed first at age 6-7 y and documented by X-ray at age 9 y (Fig. 1e; see below).

At age 15 y, the patient was nonverbal and non-communicative. On exam, he was uncooperative and restless. His weight (39.2 kg, 1st centile, Z = −2.42) and height (159.1 cm, 7th centile, Z = −1.46) were low (Fig. 1d). His head was of normal shape and size (OFC 54 cm, 25th centile). He had mild facial dysmorphism including triangular facies, anteverted nares, and micrognathia (Fig. 1a). Ears, eyes, and mouth were normal, although the mouth was held open. The neck, chest, lung, heart, abdominal, and skin were unremarkable. His genitalia were normal Tanner stage IV. Scoliosis was noted. There was striking bilateral anterior tibial bowing (Fig. 1b-c, e). The femurs were also bowed, left greater than right. The feet were flat and markedly pronated (Fig. 1b-c). He had normal upper extremities with the exception of long fingers. Neurological exam demonstrated grossly intact cranial nerves, normal strength, deep tendon reflexes, and sensation. Muscle bulk was decreased. There were no cerebellar signs. Family history was significant only for ID in a paternal first cousin once removed.

X-rays of the lower legs at age 9 y demonstrated bilateral anterior bowing of the tibias and fibulas (Fig. 1e). The diaphyses of the tibiae demonstrated hyperostosis. As bowing would not be expected with thickened cortices, the defect is a diaphyseal dysplasia. Diffuse osteopenia, non-weight-bearing pes cavus, and muscle atrophy were also seen. The growth plates appeared normal. A chest X-ray at age 6 y demonstrated mild curvature of the mid-thoracic spine with convexity to the left (Fig. 1f). A DXA scan at age 14 demonstrated osteopenia of lumbar vertebrae L1-L4 (0.803g/cm^3, Z score = −1.7; Fig S1). A brain MRI age 3 y (Fig. 1g) showed slight cerebellar tonsillar ectopia without frank Chiari-I malformation, generous subarachnoid CSF space at the plane of the foramen magnum, marked T2 bright signal around the trigones of both lateral ventricles, and shortening of the splenium of the corpus callosum. Cerebellar atrophy or other cerebellar pontine degeneration was not seen. The maxillary sinuses and ethmoid air cells contained sinus mucosal thickening. An MR spectroscopy at age 3y (Fig. S2) demonstrated a broad lipid peak centered around 1.35 ppm, which may reflect an abnormality of myelination.

In infancy, plasma amino acids, urine organic acids, quantitative screen for mucopolysaccharidoses, sterol panel, and gas chromatography mass spectrometry were normal. Anti-neuronal cell antibodies were elevated on four occasions between 4 y 5 m and 6 y 1 m (76-301 U; normal 0-54). At age 13 y, elevated serum binding antibodies to folate were identified (6.65 pmol IgG/mL), which was consistent with but does not confirm cerebral folate deficiency. Beginning at age 13 y, bone laboratory abnormalities were identified: elevated alkaline phosphatase (1,063 IU/L with 89% bone fraction at 13y and 873 IU/L at 14y; normal 107-340); elevated urinary N-telopeptide/creatinine ratio (2,885 nmol BCE/mM Cr at age 14 y; normal for Tanner IV males <609); high urinary N-telopeptide (31,610 nmol BCE at age 14 y); elevated osteocalcin (77 ng/mL at age 13 y and 105.1 ng/mL at age 14 y; normal 3.2-39.6); and elevated phosphate (4.9 mg/dL at age 13; normal 2.5-4.5). 1-, 25-OH vitamin D was normal at age 13 y (67 pg/mL; normal 10-75), but high at age 14 y (186 pg/mL). Serum calcium, calcitonin, parathyroid hormone, and 25-OH vitamin D were normal. Other laboratory values are in Table S1. A karyotype, telomere FISH, and

Angelman/Prader-Willi methylation assay at age 2 y were normal, as was a chromosomal microarray . Exome sequencing showed a heterozygous *SATB2* mutation. This mutation (c.2018dupA; p.(H673fs); hg19 chr2:200,137,118) in exon 11 (transcript NM_001172509.1) is expected to shift the reading frame. The mutation and zygosity were confirmed by Sanger sequencing, and sequencing parental DNA showed it was apparently *de novo* (Fig. S3a). No other deleterious mutations in disease genes related to the patient's phenotype were found (Table S1).

After discussions with the family, the patient was started on denosumab (Prolia) at age 16 y. He has received two subcutaneous 60 mg doses, 6 months apart, with no apparent side effects. Bone laboratory studies performed 3-4 months after the first dose were similar to prior values (calcium 9.8 mg/dL, phosphorus 5.0 mg/dL, osteocalcin 81 ng/mL, PTH 37 pg/mL, alkaline phosphatase 813 IU/L); C-telopeptide was normal at 1,514 pg/mL (normal 435-2,924). Markers just prior to the second dose (age 17 y) were also similar (calcium 10.2 mg/dl, phosphorus 5.4 mg/dl, osteocalcin 66 ng/mL, PTH 37 pg/ml, alkaline phosphatase 965 IU/L, calcitonin <2 pg/ml, 25-OH vitamin D 30 mg/ml). C-telopeptide was elevated at 3,165 pg/ml, as was procollagen type I intact N-terminal propeptide (PINP) (1,470 mcg/ml; normal 22-87 mcg/ml for males >18yo; no pediatric reference values exist).

The results described here are not considered research at our institution and therefore IRB review was not required.

DISCUSSION

We report a boy with a (c.2018dupA; p.(H673fs) mutation in *SATB2* with cleft palate, apparent ID, mild facial dysmorphism, low weight, and bone features including osteoporosis, fractures, progressive tibial bowing, and scoliosis. While cleft palate, ID, and faciodental abnormalities are typical among individuals with *SATB2*deletions, additional bone features are rare. In contrast, bone findings have been reported in five patients (including the present report) with other mutation types [Leoyklang et al., 2007; Lieden et al., 2014; Zarate et al., 2015].

Molecular evidence exists to support a genotype-phenotype correlation. The predicted consequence of the present patient's mutation is an alteration of the final five amino acids of the SATB2 homeodomain (normally encoded by amino acids 614-677) and truncation after ten additional aberrant amino acids (Fig. S3b); however, the predicted truncating codon is in the final exon of *SATB2*, so escape from nonsense-mediated decay may occur. Since all SATB2 domains would be intact except the homeodomain (Fig. S3), a dominant negative protein could result. Leoyklang et al. [2007] found that the mutant RNA in that patient (c.715C>U; p.(R239X)) was present despite an aberrant stop codon in exon 7 —, and truncated SATB2 (amino acids 1-238) had a dominant-negative effect on the wild-type protein *in vitro* [Leoyklang et al., 2013]. These data suggest that dominant negative function is a potential cause of additional bone phenotypes seen in our patient and the patient described by Leoyklang et al. [2007]. We did not obtain RNA nor assess dominant negative activity of p.(H673fs) SATB2.

Yet, evidence against a phenotype specific to truncating point mutations exists. A patient with a damaging *SATB2* point mutation (also c.715C>T; p.(R239X)) was described with no bone features [Döcker et al., 2014], and a patient with a *SATB2* deletion was found to have tibial bowing [de Ravel et al., 2009], although radiographs and bone studies were reported in neither patient. Perhaps, then, bone features are an age-dependent phenotype of *SATB2* haploinsufficiency (all patients with tibial bowing have been teenagers or older (ages 15-36), while most reported patients with *SATB2* deletion and the point mutation patient described by Döcker et al. [2014] (age 3 y) were young). Yet, deletion patients as old as 21 y [Rosenfeld et al., 2009] have been free of long bone features (see Balasubramaniam et al. [2011]), indicating that more research is needed to resolve this question. Regardless, a thorough chronology of bone involvement in the present patient shows it is a progressive phenotype.

The role of *SATB2* in skeletogenesis is supported by animal and *in vitro* studies [Zhao et al., 2014]. Despite this work, the mechanism leading to bone defects in the present patient is unknown. We found elevations in alkaline phosphatase with elevated bone fraction (a marker of osteoblastic activity or bone remodeling), urinary N-telopeptide/creatinine ratio (indicative of bone resorption/remodeling/osteoclastic activity), and osteocalcin (released by osteoblasts and present in states of increased remodeling). These values support increased turnover as the reason for this patient's progressive bone abnormalities.

We administered the osteoclast inhibitor denosumab (Prolia), a human monoclonal antibody against RANKL, to the patient. Prolia has no approved indications in children; thus, its use was off-label. Case reports of complications from denosumab in children, including life-threatening hypercalcemia after discontinuation (reviewed by Sestu et al. [2016]), warrant extremely judicious use. Of four patients with rebound hypercalcemia, all were younger (8-10 y) than the present patient and three received Xgeva, a higher dose and more frequently administered denosumab formulation [Boyce et al., 2012; Gossai et al., 2015; Grasemann et al., 2013; Setsu et al., 2016; US Food and Drug Administration 2014b]; thus, the risk to the patient reported here is unknown. He has tolerated a single dose well, experiencing no hypocalcemia or elevated PTH (known side-effects during treatment [US Food and Drug Administration 2014a]) and no rebound hypercalcemia 6 months after the first dose. An increase in C-telopeptide and an elevated P1NP at 6 months, compared with 3-4 months after the first dose, may suggest a return toward baseline levels or rebound beyond them; pre-treatment values for these markers are not available. In the future, long acting bisphosphonates will be considered.

In summary, we report a final-exon frameshift mutation in *SATB2* in a 15-year-old patient with cleft palate, apparent ID, mild facial dysmorphism, and low weight with additional features of osteoporosis, fractures, progressive tibial bowing, and scoliosis. This report provides further evidence of a single-nucleotide, potentially dominant-negative *SATB2* allele in association with phenotypes beyond those typically associated with deletion of the gene. Alternatively – or in addition – the natural history of bone suggests age-dependent penetrance. Bone laboratory makers indicate a state of increased bone turnover. Thus, we propose surveillance and treatment with anti-resorptive agents to prevent fractures and further deformity in this and similar patients.

Supplementary Material

Refer to Web version on PubMed Central for supplementary material.

ACKNOWLEDGEMENTS

P.M.B. was supported by the Baylor College of Medicine Medical Scientist Training Program (T32GM007330), Wintermann Foundation, Baylor Research Advocates for Student Scientists, and by a summer internship funded by the Texas Department of State Health Services.

REFERENCES

Balasubramanian M, Smith K, Basel-Vanagaite L, Feingold MF, Brock P, Gowans GC, Vasudevan PC, Cresswell L, Taylor EJ, Harris CJ, Friedman N, Moran R, Feret H, Zackai EH, Theisen A, Rosenfeld JA, Parker MJ. 2011. Case series: 2q33.1 microdeletion syndrome–further delineation of the phenotype. J Med Genet 48:290–298. [PubMed: 21343628]

Boyce AM, Chong WH, Yao J, Gafni RI, Kelly MH, Chamberlain CE, Bassim C, Cherman N, Ellsworth M, Kasa-Vubu JZ, Farley FA, Molinolo AA, Bhattacharyya N, Collins MT. 2012. Denosumab treatment for fibrous dysplasia. J Bone Miner Res 27:1462–1470. [PubMed: 22431375]

de Ravel TJ, Balikova I, Thiry P, Vermeesch JR, Frijns J-P. 2009. Another patient with a de novo deletion further delineates the 2q33.1 microdeletion syndrome. Eur J Med Genet 52:120–122. [PubMed: 19284984]

Döcker D, Schubach M, Menzel M, Munz M, Spaich C, Biskup S, Bartholdi D. 2014. Further delineation of the *SATB2* phenotype. Eur J Hum Genet 22:1034–1039. [PubMed: 24301056]

Gossai N, Hilgers MV, Polgreen LE, Greengard EG. 2015. Critical hypercalcemia following discontinuation of denosumab therapy for metastatic giant cell tumor of bone. Pediatr Blood Cancer 62:1078–1080. [PubMed: 25556556]

Grasemann C, Schundeln MM, Hovel M, Schweiger B, Bergmann C, Herrmann R, Wieczorek D, Zabel B, Wieland R, Hauffa BP. 2013. Effects of RANK-ligand antibody (denosumab) treatment on bone turnover markers in a girl with juvenile Paget's disease. J Clin Endocrinol Metab 98:3121–3126. [PubMed: 23788687]

Leoyklang P, Suphapeetiporn K, Siriwan P, Desudchit T, Chaowanapanja P, Gahl WA, Shotelersuk V. 2007. Heterozygous nonsense mutation *SATB2* associated with cleft palate, osteoporosis, and cognitive defects. Hum Mutat 28:732–738. [PubMed: 17377962]

Leoyklang P, Suphapeetiporn K, Srichomthong C, Tongkobpetch S, Fietze S, Dorward H, Cullinane AR, Gahl WA, Huizing M, Shotelersuk V. 2013. Disorders with similar clinical phenotypes reveal underlying genetic interaction: SATB2 acts as an activator of the *UPF3B* gene. Hum Genet 132:1383–1393. [PubMed: 23925499]

Lieden A, Kvarnung M, Nilssson D, Sahlin E, Lundberg ES. 2014. Intragenic duplication--a novel causative mechanism for SATB2-associated syndrome. Am J Med Genet A 164A:3083–3087. [PubMed: 25251319]

Rosenfeld JA, Ballif BC, Lucas A, Spence EJ, Powell C, Aylsworth AS, Torchia BA, Shaffer LG. 2009. Small deletions of *SATB2* cause some of the clinical features of the 2q33.1 microdeletion syndrome. PLoS One 4:e6568. [PubMed: 19668335]

Setsu N, Kobayashi E, Asano N, Yasui N, Kawamoto H, Kawai A, Horiuchi K. 2016. Severe hypercalcemia following denosumab treatment in a juvenile patient. J Bone Miner Metab 34:118–122. [PubMed: 26056018]

US Food and Drug Administration. 2014a. Prescribing information - Prolia® (denosumab).

US Food and Drug Administration. 2014b. Prescribing information - Xgeva® (denosumab).

Zarate YA, Perry H, Ben-Omran T, Sellars EA, Stein Q, Almureikhi M, Simmons K, Klein O, Fish J, Feingold M, Douglas J, Kruer MC, Si Y, Mao R, McKnight D, Gibellini F, Retterer K, Slavotinek A. 2015. Further supporting evidence for the *SATB2*-associated syndrome found through whole exome sequencing. Am J Med Genet A 167:1026–1032.

Zhao X, Qu Z, Tickner J, Xu J, Dai K, Zhang X. 2014. The role of SATB2 in skeletogenesis and human disease. Cytokine Growth Factor Rev 25:35–44. [PubMed: 24411565]

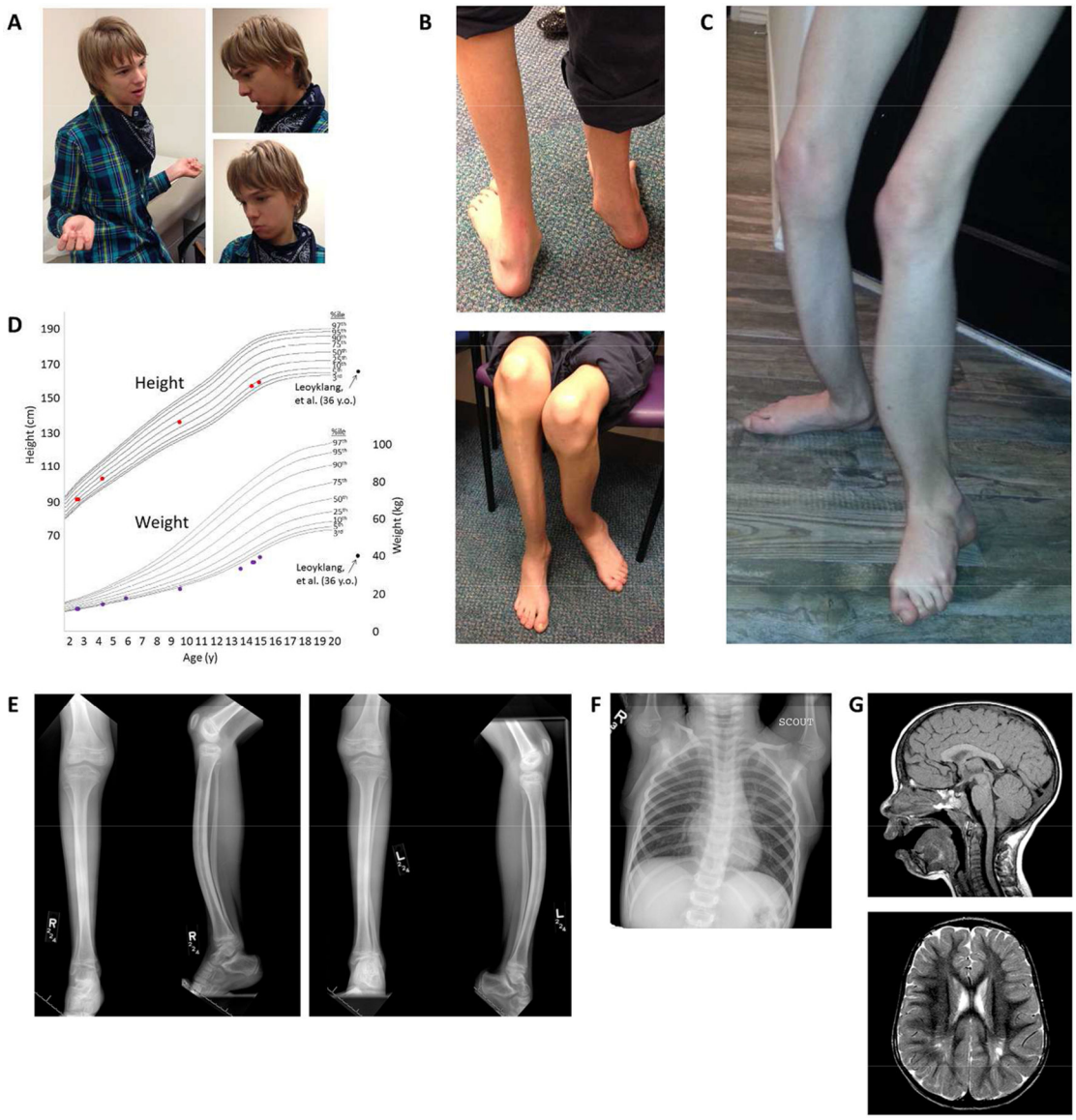

Figure 1. Physical exam findings and imaging abnormalities.

a. At age 15, mild facial dysmorphisms include triangular facies, anteverted nares, and micrognathia. **b-c.** Lower limbs with bilateral anterior tibial bowing, flat and pronated feet, and severe muscular atrophy (also at age 15 y). **d.** Growth curves demonstrating normal height (red dots), but weight (purple dots) that is low and decreasing in centile. Low weight was also present in the patients described by Leoyklang et al. [2007] and Döcker et al. [2014] (black dots). **e.** X-rays of the right (R) and left (L) lower legs (two views each) at age 9 y demonstrates anterior bowing of the tibias and fibulas with approximately 20° of angulation between the proximal and distal tibial segments. The diaphyses of the tibiae demonstrate hyperostosis. Diffuse osteopenia, non-weight-bearing pes cavus, and severe muscle atrophy are also seen. **f.** Chest X-ray at age 6 y demonstrating mild curvature of the mid-thoracic spine with convexity to the left (Cobb angle 15°). **g.** An MRI of the brain at age 3 y shows thinning of the splenium of the corpus callosum with evidence for cerebellar

tonsillar ectopia (top, sagittal T1-weighted image) and gliosis of the bilateral posterior centra semiovale with associated dilation of the perivascular spaces (bottom, axial T2-weighted image).